GEOLOGIC INTERPRETATIONS OF ELEVATED-MN CHEMCAM TARGETS IN THE BRADBURY RISE, GALE CRATER, MARS. J. M. Comellas[1], A. Essunfeld[1], N. Lanza[1], P. J. Gasda[1], D. Delapp[1], R. C. Wiens[1], O. Gasnault[2], S. Clegg[1], C. Bedford[4,5], E. Dehouck[6], B. Clark[7], R. Anderson[3], W. Fisher[8], V. Lueth[9]. [1]LANL, [2]IRAP, Toulouse, France, [3]USGS, [4]LPI, [5]NASA JSC, [6]Univ. Lyon, [7]SSI, [8]Caltech, [9]NMT.

Introduction: The presence of Mn-rich rocks on Mars could be evidence for higher concentrations of free atmospheric oxygen on ancient Mars [1]. In the terrestrial rock record, Mn-bearing rocks track the rise in atmospheric oxygen, thus acting as an indicator for redox potential of the Earth's surface [2]. MnO is not seen in Earth's geologic record until after the Great Oxidation Event due to oxygenic photosynthesis of microbial life on Earth [2].

In the first ~760 sols of the NASA *Curiosity* rover's traverse through Gale crater, *Curiosity* explored the Bradbury formation within Aeolis Palus [3]. This section of the traverse is interpreted as covering a variety of sedimentary units including aeolian, fluvial, and lacustrine deposits [3]. The Bradbury Formation has been interpreted to be a fluvial system at the distal end of an eroded alluvial fan deposit incised in the crater rim [3].

The ChemCam instrument onboard *Curiosity* is a laser-induced breakdown spectroscopy (LIBS) instrument, which provides elemental composition of rock targets [4,5]. ChemCam detected 567 observation points containing elevated concentrations of manganese (up to ~22 MnO wt.%) in 201 target rocks of the first 600 sols. We define "elevated" MnO as above 0.2 wt.%, the mean value for MnO in the Bradbury formation. Recently, a new ChemCam calibration model for MnO was developed [6]. The new model and the expanded understanding of the geologic history of Gale crater after exploring it for eight years warranted a deeper survey of the elevated-MnO targets in the first 600 sols of the traverse.

Methods: We developed a new ChemCam target classification system [7] based on attribute recognition of visual characteristics, rather than process-based terminology (e.g., "dark-toned and mottled" rather than "igneous"). The process used ChemCam remote micro images (RMI), which are taken with every raster to record the exact position of every LIBS observation. We used this classification system to sort the 201 elevated-MnO targets into 16 geologic facies. We numbered each facies and described it with the characteristic visual attributes produced by the classification system [7]. For example, Facies 0 is named "rough, dark-toned, fine-grained" and is populated with targets that fit that description.

Results: To search for compositional trends within facies, we plotted various major element compositions against MnO composition. No trends between MnO and other oxides on these simple binary plots were observed.

In addition, these data were plotted on A-CNK-FM diagrams, previously used to constrain the degree of alteration of martian rocks by [8] and used a MnO "heat map," where darker colors represent higher MnO content, to investigate the weathering and diagenesis of these elevated-MnO targets. Figures 1 and 2 show these diagrams for Facies 2 ("dimpled, dark-toned, fine-grained") and Group 12 ("oddballs"). All facies exhibit a clear decrease in Mn as points move away from the FM apex, illustrating a positive correlation between MnO and FeO_T+MgO. We see a negative correlation between MnO and CaO+Na_2O+K_2O. This creates a clear gradient in MnO between the FM apex and the midpoint of the A-CNK tie line. In Facies 0-2, and 8, we also observe unusually high MnO in a few points that plot in the region of typically lower MnO.

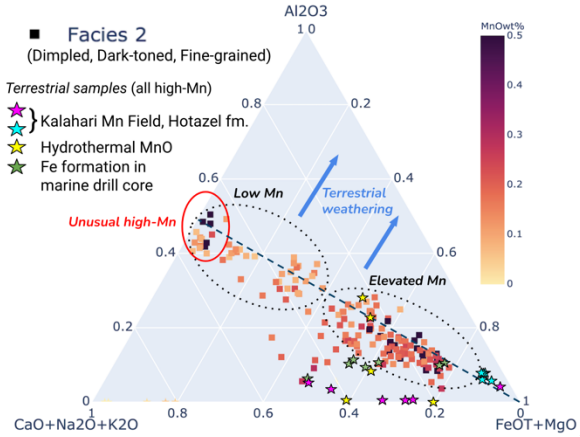

Fig. 1: Ternary diagram with Al_2O_3 (A), FeO_T+MgO (FM), and CaO+Na_2O+K_2O (CNK) apices, plotting observation points from Facies 2 (dimpled, dark-toned, fine-grained) as squares colored with a MnO wt.% heat map exhibiting distinct regions of low and high MnO. The "unusual high-Mn points" are circled in red. Terrestrial reference samples are plotted as stars. The blue arrows illustrate terrestrial weathering/open system alteration trends [8].

Stars in figures 1 & 2 represent several terrestrial samples with high Mn for comparison. Green stars are iron-rich sections of a drill core in marine shelf and deltaic sediments with on average ~6 MnO wt.% [9]. Yellow stars are sourced from Mn deposits of abiotic hydrothermal origin with on average ~30 MnO wt.% [10]. Purple and blue stars near the FM apex are "Kungara" and "Hotazel," samples from the South Africa Kalahari Manganese Field, a marine deposit associated with a banded iron formation. These two samples average ~16 MnO wt.%. Hotazel hosts Mn in two phases: braunite $[Mn(III)_6Mn(II)(SiO_4)O_8]$ and kutnohorite $[(CaMn(II)_{0.7}Mg_{0.3})(CO_3)_2]$ [11]. Most of the terrestrial samples plot below the olivine dissolution line, while some, like the hydrothermal MnO and the iron-rich drill core points, plot in the center on the "Elevated Mn" region.

Discussion: We observed no trends in binary oxide plots; hence, we inferred that there is no apparent correlation between visual appearance and the relationship between Mn and other major elements. This supports the possibility that martian Mn exists in an oxide phase.

The bulk of the data shown on the A-CNK-FM ternary (*Fig. 1)* is plotting along the dotted line between the FM

apex and the midpoint of the A-CNK tie line. This dotted line connects two end members: (end member 1) olivine, pyroxene, basaltic glass, and Fe-oxides (on the FM apex) and (end member 2) feldspar (midpoint of A-CNK tie line) [8] and represents the mafic-felsic line. Mn is known to be relatively abundant in Martian olivine and pyroxenes [e.g., 11], which could be a possible explanation for the elevated Mn points close to the FM apex. As described in [8], another possible interpretation is that points that are situated above the mafic-felsic line are altered due to the dissolution of mafic materials, and points below this line are unaltered. The points that plot toward the CNK apex (blue arrow, *Fig. 2*) are associated with secondary addition of diagenetic materials (e.g., Ca-sulfate, NaCl, etc.).

What is puzzling is the presence of unusually high Mn near the feldspar endmember (*Fig. 1*). Mn does not partition into feldspar in a melt as much as in pyroxene and olivine [e.g., 12], so there must be some other mechanism to concentrate Mn in these particular targets. A likely mechanism for concentrating Mn in these unusually high Mn observation points at low Fe and Mg (left side of *Fig. 1*) is one where a Mn-rich fluid depleted in Fe and Mg was deposited during a secondary fluid event.

The ChemCam target "Rapitan" (*Fig. 3*), an "oddball" in our visual classification system, consists primarily of calcium sulfate with several dark-toned regions of elevated Mn between the crystals. This suggests the fluid that deposited the calcium sulfate also deposited Mn, supporting the hypothesis of multiple Mn-bearing secondary fluid events, decoupled from the initial weathering of basaltic materials. However, other possibilities to explain the dark material between the calcium sulfate, such as sediment displacement [13] or a fluid event that deposited Mn, separate from the deposition of calcium sulfate, cannot be ruled out. Elevated Mn near calcium-sulfate deposits was also observed in several other targets in the oddball group.

The Mn-bearing carbonate phase of the terrestrial sample Hotazel is diagenetic in origin [8]. In the Hotazel Formation, Mn carbonates were deposited from the oxidation of carbon and reduction of Mn oxides in pore fluids [9]. Many of these Hotazel points plot near Rapitan points 1, 3, and 7 (*Fig. 2*). Though the Mn phase for the martian samples is unknown, this similarity in composition could be used as a starting point for further investigation of the formation process of targets like Rapitan.

On Mars, we see Mn-rich fracture fills [1] and potential concretions [14, 15] throughout Gale crater. Thus, we understand that this is a relatively common phenomenon on Mars. Out results are consistent with these other studies.

Conclusions: The observed relationship between calcium-sulfate and elevated Mn supports the hypothesis that Mn was deposited in several targets, sometimes along with other soluble elements, such as Ca, in multiple diagenetic events subsequent to the original dissolution of basaltic materials. The elevated-Mn points that fall near the CNK apex (*Fig. 2*) may have hit material that was once a diagenetic fluid containing both Ca and Mn which then separated at deposition, possibly due to differences in solubility. This leads us to conclude that Mn deposition may be decoupled from rock weathering. This abstract supports the claim that it is likely that there were multiple early- and late-stage fluid events in Gale crater [15].

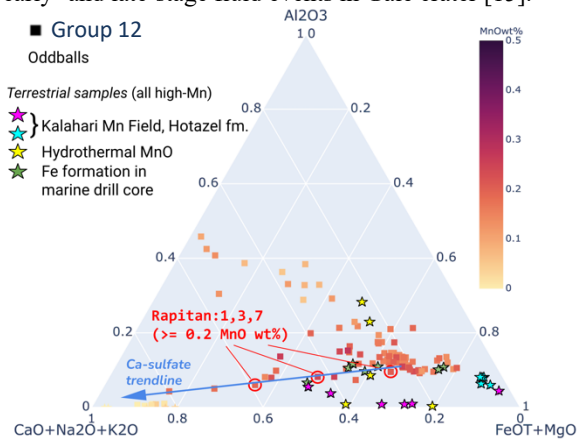

Fig. 2: Ternary diagram with Al_2O_3 (A), FeO_T+MgO (FM), and CaO+Na_2O+K_2O (CNK) apices, plotting observation points from Group 12, the "oddballs," as squares with MnO wt.% heatmap. The points highlighted in red are the high-Mn points in the target Rapitan (see Fig. 3). Terrestrial reference samples are plotted as stars. The blue arrow represents the trendline for calcium sulfate.

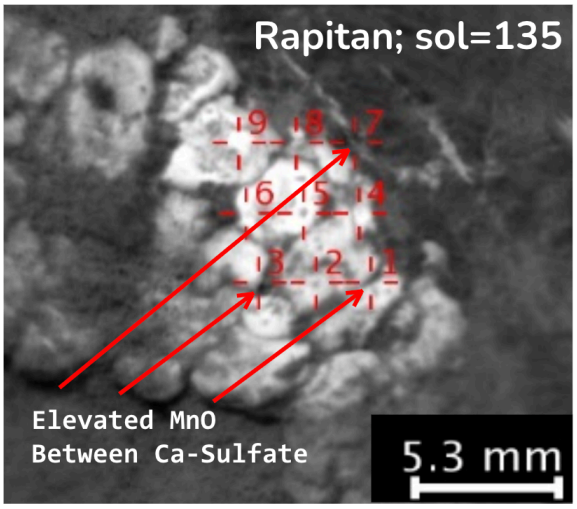

Fig. 3: Cropped RMI of the ChemCam target Rapitan from sol 135. The red arrows point to the areas between the Ca-sulfate that show elevated MnO (see Fig. 2).

Acknowledgments: NASA Mars Exploration program and CNES, France.

References: [1] Lanza N. (2016) *Geophysical research letters*,43(14), 7398-7407, [2] Maynard, J. B. (2010) *Economic Geology,* 105(3), 535-552, [3] Grotzinger (2015) *Science,* 350, 6257, aac7575, [4] Wiens et al. (2012) *SSR*, *170*:167–227, [5] Maurice et al. (2012) *SSR*, *170*:95-166. [6] Gasda et al., (2021a) *this meeting* [7] Essunfeld et al., (2021) *this meeting* [8] Hurowitz J. A. (2006) *JGR,* 111, E02S19, [9] Johnson J. E. (2013), *PNAS,*110 (28), 1238-112, [10] Norman, D.I. (1983), *34th Fall Field Conference Guidebook*, 241-246, [11] Papike et al., 2009, GCA, [12] Le Roux et al (2011). EPSL, 307(3–4), 395–408, [13] Nachon et al (2014) JGR, [14] Lanza et al (2021) this meeting, [15] Gasda et al., (2021b) *this meeting.*